(2)

OFFICE OF NAVAL RESEARCH

Grant N00014-90-J-1193

TECHNICAL REPORT No. 11

Tight-Binding and Hückel Models of Molecular Clusters

by

Daniel A. Jelski, Thomas F. George and Jean M. Vienneau

Prepared for Publication

in

Clusters of Atoms and Molecules, Chapter 2.2
Edited by H. Haberland
Springer-Verlag, Berlin

Departments of Chemistry and Physics
State University of New York at Buffalo
Buffalo, New York 14260

May 1990

UNCLASSIFIED
SECURITY CLASSIFICATION OF THIS PAGE

REPORT DOCUMENTATION PAGE

Form Approved
OMB No. 0704-0188

1a. REPORT SECURITY CLASSIFICATION Unclassified	1b. RESTRICTIVE MARKINGS
2a. SECURITY CLASSIFICATION AUTHORITY	3. DISTRIBUTION/AVAILABILITY OF REPORT Approved for public release; distribution unlimited
2b. DECLASSIFICATION/DOWNGRADING SCHEDULE	
4. PERFORMING ORGANIZATION REPORT NUMBER(S) UBUFFALO/DC/90/TR-11	5. MONITORING ORGANIZATION REPORT NUMBER(S)
6a. NAME OF PERFORMING ORGANIZATION Depts. Chemistry & Physics State University of New York 6b. OFFICE SYMBOL (If applicable)	7a. NAME OF MONITORING ORGANIZATION
6c. ADDRESS (City, State, and ZIP Code) Fronczak Hall, Amherst Campus Buffalo, New York 14260	7b. ADDRESS (City, State, and ZIP Code) Chemistry Program 800 N. Quincy Street Arlington, Virginia 22217
8a. NAME OF FUNDING/SPONSORING ORGANIZATION Office of Naval Research 8b. OFFICE SYMBOL (If applicable)	9. PROCUREMENT INSTRUMENT IDENTIFICATION NUMBER Grant N00014-90-J-1193
8c. ADDRESS (City, State, and ZIP Code) Chemistry Program 800 N. Quincy Street Arlington, Virginia 22217	10. SOURCE OF FUNDING NUMBERS PROGRAM ELEMENT NO. / PROJECT NO. / TASK NO / WORK UNIT ACCESSION NO.

11. TITLE (Include Security Classification)
Tight-Binding and Huckel Models of Molecular Clusters

12. PERSONAL AUTHOR(S)
Daniel A. Jelski, Thomas F. George and Jean Vienneau

13a. TYPE OF REPORT	13b. TIME COVERED FROM ____ TO ____	14. DATE OF REPORT (Year, Month, Day)	15. PAGE COUNT
		May 1990	37

16. SUPPLEMENTARY NOTATION Prepared for publication in Clusters of Atoms and Molecules, Chapter 2.2, Edited by H. Haberland, Springer-Verlag, Berlin

17. COSATI CODES		
FIELD	GROUP	SUB-GROUP

18. SUBJECT TERMS (Continue on reverse if necessary and identify by block number)
TIGHT-BINDING MODEL
HÜCKEL MODEL, Huckel
MOLECULAR CLUSTERS
SILICON CLUSTERS
METALLIC CLUSTERS
JG

19. ABSTRACT (Continue on reverse if necessary and identify by block number)

The background of the theory underlying the tight-binding and Hückel models of molecular structure is briefly discussed. A description is then provided for how these methods have been used in cluster research, concentrating first on applications of the tight-binding model to silicon clusters, and then on applications of the Hückel model to metallic clusters. Comments are provided on the relative merits of the two methods.

20 DISTRIBUTION/AVAILABILITY OF ABSTRACT	21. ABSTRACT SECURITY CLASSIFICATION
☒ UNCLASSIFIED/UNLIMITED ☒ SAME AS RPT. ☐ DTIC USERS	Unclassified
22a. NAME OF RESPONSIBLE INDIVIDUAL Dr. David L. Nelson	22b. TELEPHONE (Include Area Code) (202) 696-4410 22c. OFFICE SYMBOL

DD Form 1473, JUN 86 *Previous editions are obsolete.*

SECURITY CLASSIFICATION OF THIS PAGE
UNCLASSIFIED

Clusters of Atoms and Molecules, Chapter 2.2
Edited by H. Haberland
Springer-Verlag, Berlin, 1990

Chapter 2.2: TIGHT-BINDING AND HÜCKEL MODELS OF MOLECULAR CLUSTERS

Daniel A. Jelski
Department of Chemistry
State University of New York, College at Fredonia
Fredonia, New York 14063
U.S.A.

Thomas F. George
Departments of Chemistry and Physics & Astronomy
239 Fronczak Hall
State University of New York at Buffalo
Buffalo, New York 14260
U.S.A.

Jean M. Vienneau
Department of Chemistry
State University of New York, College at Fredonia
Fredonia, New York 14063
U.S.A.

Abstract

The background of the theory underlying the tight-binding and Hückel models of molecular structure is briefly discussed. A description is then provided for how these methods have been used in cluster research, concentrating first on applications of the tight-binding model to silicon clusters, and then on applications of the Hückel model to metallic clusters. Comments are provided on the relative merits of the two methods.

2.2.1. Introduction

We now consider a simplified method for calculating electronic states of clusters. In the next chapter, local density calculations originally developed for the bulk metal are adapted for cluster calculations. This results in a "solid" in which surface effects are important. Similarly, Hartree-Fock methods are frequently used to calculate the structure of small molecules and clusters. In the current chapter, we shall not be concerned with solving the Schrödinger equation from first principles, but shall instead adopt a semiempirical approach. Apart from computational simplicity, the benefits of this approach are several-fold. First, surface effects are automatically taken care of. Secondly, the geometry of the cluster can be given explicitly, and there is no need to assume a spherical or model geometry. Finally, the electronic structure can be probed more accurately, since the electronic states are calculated explicitly.

The limitations of the present method must also be explored. In particular, the semiempirical parameters are usually calculated from the band structure in the bulk. There is no guarantee that this parametrization will continue to be valid for very different cluster systems. In any event, some modification of the method must be undertaken before these methods can be applied to clusters. Secondly, while some information about the electronic structure is inherent in any method which depends on the bulk band gap, how accurate that information is for systems different from the bulk and/or for states not near the band gap remains to be determined. Finally, one is limited to materials for which suitable parameters are known, and for which a variety of approximations are appropriate. Nevertheless, there are many systems for which quantum chemical techniques can yield valuable information,

and the purpose of this chapter is to indicate that many of the above problems are soluble.

We should distinguish the present techniques from classical force field methods. These methods attempt to model the potential around an atom using a classical field, and from this to calculate stable structures and heats of formation from molecular dynamics calculations. This is very widely used in cluster research and yields much valuable information, but it is beyond the scope of this chapter. Since it is not a quantum mechanical method, little information about electronic structure can be obtained.

The most straightforward quantum technique is, of course, the ab initio Hartree-Fock calculation. In this case the Schrödinger equation is solved explicitly, and solutions of arbitrary accuracy can be obtained, depending on the size of the computer and the patience of the researcher. Most ab initio calculations are done for small molecules, and the amount of computation involved makes this method inappropriate for larger systems.

Short of ab initio techniques, there exists a large number of semiempirical methods. These begin with the principles of quantum mechanics, but then greatly simplify the calculation by introducing empirical parameters, which are chosen to produce as accurate a result as possible. In many cases the results are very accurate indeed, and it is not always fair to say that semiempirical methods are less exact than ab initio techniques. Semiempirical methods are widely used in studies of organic systems. Pharmaceutical firms make much use of these methods in searching for new drugs.

The methods we are about to describe are semiempirical of the simplest sort, involving only one or a few parameters. Their great advantage is computational and conceptual simplicity, and they are readily adaptable to

calculations of large clusters. Specifically, in what follows we shall consider the tight-binding model and the Hückel model. Both of these are so-called nearest-neighbor models, in which the interaction between nearest-neighboring atomic sites is accounted for, and all other interactions are ignored.

We start with a short background of the theory underlying the two methods. We then continue with a description of how the methods have been used in cluster research, concentrating first on application of the tight-binding model to silicon clusters, and then on applications of the Hückel model to metallic clusters. Finally, we close with some comments on the relative merits of the methods, and on possible directions for future research.

2.2.2. Quantum Chemistry Background

In order to define notation, and also to ensure completeness, we review here some elementary quantum chemistry as will be used in what follows. The Hamiltonian for a molecule can be written as

$$H\psi_i = E_i\psi_i \quad , \qquad (1)$$

where ψ_i refers to a molecular electronic state with energy E_i, which are the quantities we want to determine. In principle, of course, H depends on all electron-nuclear and electron-electron interactions. But the tight-binding (TB) model assumes that the total Hamiltonian can be simplified into a series of one-electron Hamiltonians, i.e., that each electron feels an average field made up of the nuclei and all other electrons. This is the same approximation as made by the Hartree-Fock approach, but the TB method is not a self-consistent approach.

The second characteristic of the TB model is that local, atomic orbitals are used as a basis set. It is from this that the method takes its name, i.e., it is assumed that each electron is well localized around a given nucleus. The opposite standpoint would be to assume plane-wave Bloch functions for the basis set, which is the approach used for many metals. Bullett[1] has shown that by including d-orbitals, the TB basis set looks more and more like the plane-wave approach, and thus can be used for metals as well. Our discussion here, however, restricts attention to s and p orbitals, and hence the TB method described here is not applicable to systems such as metals where electrons are nearly free.

We can write the one-electron states as

$$H_\alpha \phi_\alpha = \epsilon_\alpha \phi_\alpha \quad , \tag{2}$$

where α refers to the one-electron, atomic Hamiltonian, energy and orbital. For an isolated atom, this is an exact expression. The ϕ_α constitute our basis set, and so we can express the molecular orbitals in terms of them as

$$\psi_i = \sum_\alpha c_{i\alpha} \phi_\alpha \quad . \tag{3}$$

Operating on this with the molecular electronic Hamiltonian, H, we get

$$H\psi_i = H\left(\sum_\alpha c_{i\alpha} \phi_\alpha\right) = E_i \psi_i \quad . \tag{4}$$

We can rewrite Eq. 4 using Dirac notation as

$$H|i\rangle = \sum_{\alpha} c_{i\alpha} H|\alpha\rangle = E_i|i\rangle \quad . \tag{5}$$

From this, the energy E_i can be written as

$$E_i = \sum_{\alpha,\beta} c^*_{\beta i} c_{i\alpha} \langle\beta|H|\alpha\rangle = \sum_{\alpha,\beta} c^*_{\beta i} c_{i\alpha} V_{\beta\alpha} \quad , \tag{6}$$

where Greek letters refer to atomic states, and where $V_{\alpha\beta}$ is the numerical value of the integral expressed by the brackets.

Equation 5 is a system of n equations with n unknowns, where n is the size of the basis set, in principle infinite. We can rewrite Eq. 5 in determinantal form

$$\det|H - E_i S| = 0 \quad , \tag{7}$$

where S refers to the overlap matrix, and H refers to the Hamiltonian matrix given by Eq. 5. For an orthogonal basis set, S is simply a unit matrix. For a non-orthogonal basis set, S must be calculated explicitly. However, in our derivation we will assume that ϕ_α and ϕ_β are orthogonal, i.e., that $\langle\alpha|\beta\rangle = 0$ for $\alpha \neq \beta$, and thus $S_{\alpha,\beta} = \delta_{\alpha\beta}$. This is obviously true if the orbitals are on the same atom, since hydrogen-like orbitals are orthogonal. It is not true if the orbitals are on different atoms, since it is precisely the overlap which creates the bond. But since the overlap is generally small, it can be included in the parametrization, and therefore ignored. Simplicity demands such a procedure, and it is the course we follow here. A more detailed account is found in Bullett's review article.[1]

The second approximation is to assume that the molecular electronic Hamiltonian acts on the atomic orbital as

$$H|\alpha\rangle = H_\alpha|\alpha\rangle = \epsilon_\alpha|\alpha\rangle \quad . \tag{8}$$

This is the same as saying that the molecular electronic Hamiltonian for an isolated atom is the same as the atomic Hamiltonian from which the basis set is derived. A more mathematically sophisticated way of saying this is to use projection operators, as discussed by Bullett.

The final approximation is to note that

$$\begin{aligned} \langle\beta|H|\alpha\rangle = V_{\beta\alpha} &= 0 \quad \text{for } \alpha,\beta \text{ on same atom, or on distant atoms} \\ &\neq 0 \quad \text{for } \alpha,\beta \text{ on nearest-neighbor atoms.} \end{aligned} \tag{9}$$

This is how the interaction between atoms in the molecule is taken into account. In general, of course, $V_{\beta\alpha}$ has to depend on the interatomic distance, and the TB model does that. In the present case, $V_{\alpha\beta}$ is calculated for a fixed interatomic distance, and then is allowed to vary as $1/r^2$.

The parameters for silicon are well known: $V_{ss\sigma} = -1.938$ eV, $V_{sp\sigma} = 1.745$ eV, $V_{pp\sigma} = 3.050$ eV and $V_{pp\pi} = -1.075$ eV.[2] These have been calculated to fit the band structure of the bulk material, and have no other immediate physical significance other than that they work. At large distances, the decay is much faster than $1/r^2$, and therefore a cutoff distance is chosen after which the matrix elements are set to zero, and no bond is said to exist. In addition, we include the diagonal terms of the matrix in Eq. 7, which are

adjusted so that an isolated atom in the ground state is at zero energy. These are E_s = -5.25 eV and E_p = 1.20 eV.

Equation 7 can then be solved. Each bond is projected along the x, y and z coordinates, and then weighted according to the interatomic distance. The matrix is then diagonalized. The eigenvalues correspond to the energy levels, and the eigenvectors are the coefficients, $c_{i\alpha}$. The value $c^*_{i\alpha}c_{\alpha i}$ corresponds to the contribution of atomic orbital i to molecular orbital α, or, the probability of an electron in molecular orbital α being in atomic orbital i. In the model which we have presented, the matrix to be diagonalized is real and symmetric, and therefore all eigenvalues and eigenvectors are real.

Similarly, the sum $\sum_\alpha c^*_{i\alpha}c_{\alpha i}n_\alpha$ is the total charge density in atomic orbital i, where n_α is the occupation number of molecular orbital α. In the case of s and p orbitals, there are four orbitals per atomic site, and thus the total charge on a given atom (labelled k) as a result of an electron in molecular orbital α is

$$q_k = \sum_{i \text{ on } k} \sum_\alpha n_\alpha c^*_{i\alpha}c_{\alpha i} \quad . \tag{10}$$

The evaluation of Eq. 10 is known as a Mulliken population analysis, and from it one can gather information not only about the energy of a cluster, but also about the charge distribution. Such data must be handled with care, however, as will be illustrated in the next section.

The Hückel model differs from the general TB model in two respects.[3] First, instead of including s and p orbitals in the basis set, it only includes s orbitals. Hence the assumption is that there is only one valence

electron per atom. This means that there are only two parameters, the diagonal terms, known as the Coulomb integral, usually abbreviated as α, and the off-diagonal terms, corresponding to the V_{ss} interaction between nearest neighbors, which is denoted by β and termed the resonance integral. Since the s orbital is spherically symmetric, there is no angle dependence in the model. Further, in the simplest case, there is no length dependence on β, and so the result depends only on topology. However, it is a relatively simple matter to include a distance-dependent term, in which case the Hückel model is extended and more accurate.

2.2.3. Application to Clusters

The parameters given above are fitted to solid silicon in a diamond lattice structure.[2] They are chosen to match the band structure for that system. The self-energy terms, E_s and E_p, are chosen so that the zero-point energy is the Fermi level of the solid. It is not entirely clear that the above model holds for clusters, and in any event, some additional features must be considered.

In the first case, the bulk parameters are chosen for the equilibrium geometry, i.e., a fixed system. This is easy since all bonds and atoms in the lattice are identical. But for clusters, it is necessary to accommodate varying bond lengths. For this, some reasonable potential must be included. Tománek and Schlüter[4] have done this by using an analytic expression for the silicon dimer, matched to ab initio results. This is used to develop a repulsive potential curve. The attractive part of the potential is fitted by multiplying the TB parameters by $1/r^2$, while continuing to insist that the band structure of the bulk comes out properly. Thus the repulsive part of the

potential is assumed to be a pair-wise classical potential, whereas the attractive part comes from the band structure calculation.

The second problem in using the model for clusters comes from the varying coordination numbers. In the bulk, all atoms are tetrahedrally coordinated, and hence it is not necessary to account for energy differences arising from this source. But for a cluster, this can yield important variations. Thus it is necessary to include a parametrization which depends on the ratio between bonds and atoms. Tománek and Schlüter have done this by fitting a quadratic equation to the dimer and two bulk structures, diamond and fcc. This equation is

$$E_{CN} = n[\chi_1(n_b/n)^2 + \chi_2(n_b/n) + \chi_3] \quad , \qquad (11)$$

where n refers to the total number of atoms, and n_b to the total number of bonds. The χ_i's are empirically fitted.

The final problem in applying the TB model to clusters concerns charge separation. For the solid lattice this difficulty does not arise (at least for a homonuclear species like silicon), but for clusters, it is necessary to account for the fact that there may be a dipole moment. Thus Coulomb forces must be accounted for explicitly. Tománek and Schlüter have done this by including $U(q_k^2 - q_0^2)$ in the Hamiltonian, where q_k is calculated from Eq. 10, and q_0 is the number of valence electrons on a neutral silicon atom. The constant U is to be empirically determined, but in the absence of data with which to fit it, it is chosen as unity.

Thus the complete Hamiltonian to be applied to clusters is[4]

$$E_{coh} = \sum_{\alpha} n_{\alpha} E_{\alpha} - \sum_{\sigma} n_i E_i + \sum_{k \neq j} \sum E_{repulsive}(j,k) + E_{CN} + \sum_{k} U(q_k^2 - q_0^2), \quad (12)$$

where the first term on the rhs is the band energy. The second term sets the zero energy to an isolated atom in the ground state, so that the resulting energy is the cohesion energy of the cluster, E_{coh}. E_{CN} is the bond-number-dependent term from Eq. 11, and the last term is the Coulomb term. The above Hamiltonian is fitted to match the bulk and the dimer exactly, and it is hoped that it will apply to situations in between. Whether or not it does is the subject of the next section.

2.2.4. TB Model Applied to Silicon Clusters

The test of the TB model when applied to silicon clusters ultimately rests on comparison with experiment. Experimental data is more difficult to come by, and so some of our results remain speculative. Nevertheless, there is a sufficiently good match to indicate that the TB model is valid over a range of structures. Tománek and Schlüter,[4] having developed the model described above, were the first to apply it to small silicon clusters, where they compared their results with a local-density approximation calculation. While we refer the reader to the original article for the details, it may safely be said that the results largely agree, at least in terms of the cohesion energy. This constitutes the first evidence that the TB model may be useful. Tománek and Schlüter performed a calculation on two structures of Si_{10}, a tetracapped octahedron (TO, shown in Fig. 1) and an adamantane-like structure, which is a bulk fragment. The TO isomer was found to have a cohesion energy of -3.6 eV/atom, whereas the adamantane form was found to be unstable.

We have performed an extensive study of Si_{10} isomers,[5] comparing not only energies, but also whatever other experimental parameters can be culled from the literature. The various structures we found are shown in Fig. 1. We review these results with an eye toward establishing the benefits of the TB model. The most stable structure is a distorted form of a bicapped tetragonal antiprism (DBTA-I). The distortion results from Jahn-Teller effects since the ground state of undistorted BTA is degenerate. As shown in Table I, the cohesion energy of DBTA-I is -3.98 eV/atom. Equally important, the HOMO-LUMO gap is 1.4 eV. This matches very closely to the experimental value of about 1.2 eV.[6]

This result for DBTA dramatically illustrates the advantages of the TB model. In order to derive a distorted structure, global optimization is necessary. Indeed, we find another metastable structure (DBTA-II) which is also a Jahn-Teller distortion of BTA. In this instance, the HOMO-LUMO gap is 0.6 eV. An ab initio calculation can do a global optimization only with great difficulty, and classical force field approaches cannot deal with Jahn-Teller effects. Thus semiempirical techniques are best from this point of view. Ideally, however, the result can be confirmed by an ab initio calculation.

Closer consideration of DBTA-I yields more information about both the TB model and the nature of silicon clusters. Figure 2 contains information about bond lengths for various isomers. A difficulty with the TB model is that it depends on the number of bonds through Eqs. 9 and 11. This problem is usually solved by choosing a cutoff value, i.e., two atoms are considered bonded when separated by less than the cutoff value, and unbonded when further apart. This is another parameter put into the calculation, and is chosen to best match experimental evidence. Tománek and Schlüter have chosen the cutoff

value to be 0.255 nm, which is the average of nearest-neighbor and next-nearest-neighbor distances in the bulk. This value is fine as long as coordination numbers and structures are similar to those in the bulk, but it fails for clusters with coordination numbers larger than 4 or 5.

The importance of the cutoff value is shown in Fig. 2. This value is illustrated by the dashed line, and as can be seen, for most clusters a choice between 0.3 nm to 0.35 nm makes no difference and is therefore arbitrary. For DBTA-I, however, there are two atoms which are approximately 0.33 nm apart, and this provides a test for the appropriate cutoff distance. We have performed the calculation for DBTA-I under two situations, with the 24-bond version of the isomer and also with the 25-bond version. The results are given in Table I, and it can be seen that the 25-bond version more closely matches the experimental parameters. In fact, a partial bond is probably a better way of dealing with the situation, and in principle one could use some smooth curve to delineate bonded from unbonded atoms, rather than a cutoff value. Nevertheless, we now have direct evidence for appropriate bond lengths in clusters, and we are thus also able to extend the applicability of the model to larger coordination numbers.

The results in Table I are consistent with those calculated elsewhere. A classical force field model yields BTA as the most stable isomer. A calculation by Parinello and co-workers suggests a tie between the TO and TTP isomers,[7] and <u>ab initio</u> results vary between TTP and TO.[8-10] None of these calculations include Jahn-Teller effects, and none of them reproduce the experimentally observed band gap. BTA has a degenerate ground state, and TTP and TO have band gaps more than twice that observed. Further, if one assumes that the activation barrier separating the BTA related forms is very small,

then two isomers exist in equilibrium, these being DBTA and TTP, with DBTA as the most abundant species. Experimental evidence indicates that at least two isomers of Si_{10} exist with 85% and 15% population distributions.[11] This data is entirely consistent with our result.

We thus conclude that the TB model is a fairly accurate way of dealing with silicon clusters. The original parameters were chosen by Tománek and Schlüter, and we have further investigated the problem of the cutoff distance. We find that a good physical argument can be made for choosing 0.33 nm. Our relative energies are consistent with those of other workers, and our data match the PES spectra and the thermal distribution data. We thus conclude that the TB model is probably useful for investigating larger clusters.

The first larger system we have investigated is silicon cluster cations ranging from 30 to 45 atoms.[12] This was inspired by experimental evidence indicating a dramatic difference in chemical reactivity for different sized clusters.[13] Ammonia and methanol are found to react quickly with clusters containing 30, 36, 43-44 and 46 atoms, and are found to react only slowly with clusters containing 33, 39 and 45 atoms. There are two orders of magnitude separating the reactivity of Si_{36}^{+} from Si_{39}^{+}. Conversely, there is no significant variation found in reactivity with oxygen or nitrogen oxide.

Several salient points can now be mentioned. First, the periodicity in reactivity is roughly six atoms. This seems to indicate a six-membered ring as a basic unit. Secondly, the reactivity with strong free radicals (such as O_2 and NO) is non-periodic. This seems to indicate that the number of dangling bonds is not the determining factor, since free radicals would be expected to react with dangling bonds. Thus there must be some other feature of the structure which determines the reaction rate. We have used the TB

model to investigate this more closely. Since this work was done prior to the work on Si_{10}, the cutoff distance used for this study was 0.255 nm, taken from Tománek and Schlüter.

Six-membered rings of silicon atoms are stacked as shown in Fig. 3. When the number of atoms is not divisible by six, the remaining atoms are arranged as a cap at one end of the cylinder. In the first instance, we are interested in determining the stability and geometry of the structures. We find that all such structures, from n = 30 to 45 are metastable. To our surprise, we also find that the rings are quite flat. We also find that while bending increases the stability of the ring, it substantially weakens the bonds between the rings, thereby raising the energy of the cluster. The precise geometry of the clusters is given in the original reference.

The problem is to account for the difference in reactivity. Figure 4 depicts the charge distribution as a function of cluster size. Given the large variation in reactivity, we require a large qualitative difference in some property. It is observed that a three-atom cap has a negative total charge, whereas caps of other sizes tend to be positive. Exceptions are for n = 28, 29, 40 and 41, which correspond to four or five atom caps. These are also slightly negative, but are not especially reactive. The Si_{39}^{+} cluster is the least reactive, and it is the only species to be negatively charged at both ends.

Thus the charge distribution appears to vary qualitatively as a function of cluster size. If ammonia and methanol are thought of as nucleophiles, then their reactivity with a positively-charged cap is straightforward. Similarly, the reactivity with a negatively charged cap is expected to be greatly diminished. A three-atom cap tends to draw electrons toward it, and thus

tends to be negatively charged. This can be considered a resonance effect. Similarly, since the variation in dangling bonds is not qualitatively different as a function of n, it follows that free radicals react indiscriminately.

It is interesting to note that these experiments were done for the cation, which implies that a local negative charge is less likely. The prediction, therefore, is that the reactivity pattern for the neutral or anionic species will be much less pronounced since four and five atom caps would draw significant electron density.

The second project is to investigate the structure of Si_{60}^{+}. Again, the impetus is a remarkably simple experimental result, notably the photofragmentation data.[14] It is found for Si_{60}^{+}, as well as for a wide range of other sizes of silicon and germanium clusters, that the photofragmentation pattern yields predominantly Si_{10}^{+}. The experimenters point out that the charge on the original cluster is most likely to migrate to the largest fragment, and therefore the complete absence of fragments larger than 11 or 12 atoms indicates that the Si_{60}^{+} ion explodes rather than just breaking into two or several pieces.

There are two approaches which can be used here. One is to suggest that Si_{10}^{+} is more stable than other small clusters, and hence ten atoms is the preferred size. The difficulty is that this does not appear to be the case, for it appears that cohesion energy rises as a function of size (for small clusters), and further, that Si_{13} is considerably more stable than the Si_{10} fragment. The second possibility is that silicon clusters fragment into ten-atom pieces by virtue of the construction of the parent species. If this is

true, then it imposes a significant condition on the structure of clusters larger than twenty atoms.

We choose to investigate the second possibility by studying the properties of an Si_{60} cluster arranged as shown in Fig. 5, and which we describe as stacked, Si-naphthalene rings. This is the next logical step beyond stacked six-membered rings. The purpose of this exercise is to see if this constitutes a stable structure, to determine a logical fragmentation pattern, and to estimate the degree of conjugation around the rings. If fragmentation occurs between the planes, then a ten-atom fragment is a likely product.

A larger model can now be considered. For small clusters, $n < 20$, the structure is molecular in form, i.e., close-packed with large coordination numbers. Very large clusters assume a bulk structure. The difficulty arises for intermediate forms. The molecular framework does not work, since then a close-packed solid would result. Similarly, a large surface area precludes a straightforward application of the bulk model. Thus the arrangement in Figs. 3 and 5 seems reasonable. Most atoms are tetra-coordinated, the surface area is minimized, and reactivity and fragmentation patterns can be accommodated. Other models have also been proposed which solve many of the same difficulties.[15,16] The experimental art does not yet permit resolution between these conflicting theories.

The cohesion energy of the Si_{60} cluster in Fig. 5 is -3.6 eV. This compares to a bulk value of -4.4 eV, and the value for Si_{10} of -4.0 eV. This trend is consistent with the above hypothesis, since both a tightly-packed small cluster or a stable solid would be more stable than the intermediate system. The charge distribution is given in Fig. 6, which indicates that negative charge is concentrated in the center of the molecule.

Of primary interest are the bond strengths of the cluster, shown in Fig. 7. This is calculated using values for overlap integrals given by Mulliken. It can be seen that the weakest bonds are between the planes second from the ends. Thus if the cluster were to fragment, it would most likely fragment along these lines, leaving three, twenty-atom fragments. The Si_{20} fragment has a cohesion energy of -3.2 eV and is probably unstable with respect to dissociation to Si_{10}. Hence the appearance of ten-atom daughter fragments follows.

To conclude this section, we review what we have tried to do. We have used the tight-binding model to determine properties of silicon clusters. The advantages of this are that it is simple enough to allow complete geometric optimization, while still providing data about electronic states. Strong evidence for the suitability of the model is provided by the results for Si_{10}, and also by the work of Tománek and Schlüter on smaller clusters. This model has subsequently been applied to larger clusters with an eye toward explaining the reactivity and photofragmentation data.

2.2.5 Applications of the Hückel Model

We very briefly review some work using the Hückel model.[3] A Hückel calculation is valid primarily for atoms with a spherical valence shell, and thus has been used mainly for alkali metals. It was originally developed, however, to describe conjugated carbon systems, in which π electrons are considered to be valence electrons, and σ electrons are considered to be inner-shell. This approach is very primitive and is valid provided the angular dependence of the Hamiltonian can be neglected. In the simplest case, not even the radial dependence is included, though Salem indicates simply how that can be accomplished.

Our laboratory has used the Hückel model to calculate stable structures of sodium clusters.[17,18] This simple model was used so as to permit a very rapid calculation of a large number of different isomers, necessary because there are as many as 11-million ways of constructing Na_{10}.[17] Graph theory was used in analyzing this problem. This is possible because the Hückel model depends only on the adjacency matrix, and hence a molecule can be represented topologically. A scheme was developed to eliminate most isomorphic graphs. However, since graph theory does not accommodate bond lengths, a geometric constraint reduces the number of possible isomers dramatically. Thus the energies of all topologically and geometrically allowed structures were calculated using the Hückel method, both for the neutral and cationic species. This yields stable structures, a representative sample of which are shown in Fig. 8.

Some interesting data about the transition from molecule to solid now emerge. The energy spectrum can be calculated using the Hückel model.[18] It is found that this falls into certain bands which can be described by the usual s, p, and d notation, depending upon the orbital angular momenta. The band energies can be modelled by a least squares fit to the function

$$E_\ell(n) = A_\ell + B_\ell(n^{1/3} + 1)^{-2} \quad , \qquad (13)$$

where n is the number of atoms in the cluster, and A_ℓ and B_ℓ are determined from the curve fit. The subscript ℓ distinguishes between orbitals with s, p or d symmetry. This curve matches the energy spectrum very well. However, there are two breaks where the energy of the bands is significantly different. These occur at n = 7 and n = 12. At n = 7 it is observed that the cluster

structures change from two-dimensional to three-dimensional. At n = 12 it is observed that there are body atoms inside the cluster that appear to be bulk-like. Thus the breaks in the band structure can be directly correlated to the size of the cluster, and it appears that clusters with 12 or more atoms will behave more like the bulk metal.

2.2.6 Conclusions

The last paragraph is a good example of both the advantages and disadvantages of the tight-binding and Hückel model approaches. On the plus side is computational simplicity. This allows the rapid determination of a large number of structures, and also the calculation of general trends in electronic properties. This is also true with silicon clusters, where full geometric optimization is found to be important. State-of-the-art ab initio calculations are as yet unable to accomplish this.

Interest in clusters has been renewed because of their optical properties. Here data about excited states is crucial, and the tight-binding method may be able to provide this. By definition, the TB model is fitted to the band gap in the bulk, and therefore should be expected to yield accurate excited state data near the band gap. Far from the band gap is a different story, and there the accuracy of the method remains to be tested. Nevertheless, the TB method provides an excellent method of estimating optical parameters with relatively little work, and incorporating full geometric optimization.

A second virtue of the TB method is that it is readily applicable to solid state chemistry. In a sense, a cluster can be viewed as a defect in a solid. There has recently been some interesting work on lattice defects using variations on the TB model. This becomes especially interesting since it is supposed that embedded clusters will have special optical properties. The

nature of these embedding effects is something that can conceivably be investigated.

Acknowledgments

Acknowledgment is made by DAJ to the donors of the Petroleum Research Fund, administered by the American Chemical Society, for partial support of this research. DAJ also acknowledges that this research was partially supported by a grant from the Research Corporation of the State University of New York, and he thanks the SUNY Research Foundation for an Equipment Matching Grant. TFG acknowledges support by the Office of Naval Research and the National Science Foundation under Grant CHE-8620274.

References

1. D. W. Bullett, in Solid State Physics, Vol. 35, edited by H. Ehrenreich, F. Seitz and D. Turnbull (Academic, New York, 1980), pp. 129-214.

2. D. J. Chadi, Phys. Rev. B 29, 785 (1984).

3. L. Salem, Molecular Orbital Theory of Conjugated Systems (W. A. Benjamin, New York, 1966).

4. D. Tománek and M. A. Schlüter, Phys. Rev. B 36, 1208 (1987). See also P. B. Allen, J. Q. Broughton and A. K. McMahan, Phys. Rev. B 34, 859 (1986); F. S. Khan and J. Q. Broughton, Phys. Rev. B 39, 3688 (1989).

5. T. T. Rantala, D. A. Jelski and T. F. George, J. Cluster Sci, submitted.

6. O. Cheshnovsky, S. H. Yang, C. L. Pettiette, M. J. Craycraft, Y. Liu and R. E. Smalley, Chem. Phys. Lett. 138, 119 (1987).

7. P. Ballone, W. Andreoni, R. Car and M. Parrinello, Phys. Rev. Lett. 60, 271 (1988).

8. K. Raghavachari and V. Logovinsky, Phys. Rev. Lett. 55, 2853 (1985).

9. K. Raghavachari, J. Chem. Phys. 83, 3520 (1985); 84, 5672 (1986).

10. K. Raghavachari and C. M. Rohlfing, J. Chem. Phys. 89, 2219 (1988).

11. M. F. Jarrold, J. E. Bower and K. Creegan, J. Chem. Phys. 90, 3615 (1989).

12. D. A. Jelski, Z. C. Wu and T. F. George, Chem. Phys. Lett. 150, 447 (1988).

13. Y. Liu, Q.-L. Zhang, F. K. Tittel, R. F. Carl and R. E. Smalley, J. Chem. Phys. 85, 7434 (1986); J. L. Elkind, J. M. Alford, F. D. Weiss, R. T. Laaksonen and R. E. Smalley, J. Chem. Phys. 87, 2397 (1987).

14. Q.-L. Zhang, Y. Liu, R. F. Curl, F. K. Tittel and R. E. Smalley, J. Chem. Phys. 88, 1670 (1988).

15. E. Kaxiras, Chem. Phys. Lett. 163, 323 (1989); Phys. Rev. Lett. 64, 551 (1990).

16. H. Kupka and K. Jug, Chem. Phys. 130, 23 (1989).

17. Y. Wang, T. F. George, D. M. Lindsay and A. C. Beri, J. Chem. Phys. 86, 3493 (1987).

18. D. M. Lindsay, Y. Wang and T. F. George, J. Chem. Phys. 86, 3500 (1987).

Table 1

Cohesion energies, HOMO-LUMO transition energies and LUMO energies of various Si_{10} structures, shown in Fig. 1. The LUMO one-electron energy, which is a rough indication of the electron affinity, is given relative to the "HOMO" level of the bulk.

Species	Cohesion Energy (eV/atom)	HOMO-LUMO Gap (eV)	LUMO Level (eV)
DBTA-I*	-3.98 (-3.92)	1.4 (0.9)	+0.18 (+0.13)
DBTA-II	-3.92	0.6	-0.50
BTA	-3.90	0.0	-0.92**
TTP	-3.91	2.6	+1.21
TO	-3.61	2.9	+2.00

* The values for the 24-bond structure are given in parentheses.

** Since the ground state is degenerate, this is also the HOMO level.

Figure Captions

Fig. 1 Structures of various Si_{10} isomers: (a) tetracapped octahedron (TO); (b) tetracapped trigonal prism (TTP); (c) bicapped tetragonal antiprism (BTA); (d) distorted BTA-I (DBTA-I), with the possible 25th bond indicated by the dashed line. The unit on each axis is Å.

Fig. 2 Range of bond lengths for different isomers. The cutoff parameter chosen (0.33 nm) is shown by the dashed line. The thick bars below illustrate the range of bond lengths in the cluster. The thin bars above indicate the range of non-bonded distances, with the upper limit corresponding to the maximum diameter of the cluster. For DBTA-I two possibilities are indicated. On the left, the 25-bond form is shown, whereas on the right, the 24-bond form is shown. The unit on each axis is Å.

Fig. 3 Geometry of two silicon clusters, Si_{37}^{+} and Si_{39}^{+}, with a silicon atom at each vertex.

Fig. 4 Total electronic charge per layer for different silicon clusters. The diagrams on the left of each figure represent a schema of the cluster geometry, with the solid bars denoting a six-membered ring, and the individual atoms of the cap are shown explicitly. The bar graphs on the right show the total charge per layer, i.e., the sum of the charges of each atom constituting a single layer.

Fig. 5 The proposed structure for the Si_{60} cluster, consisting of six, stacked, ten-atom naphthalene-like rings.

Fig. 6 The charge density distribution in Si_{60}. Each line represents one naphthalene plane, and the number is total charge on that plane, in units of electronic charge.

Fig. 7 The average bond strength of the bonds between each of the planes in the proposed Si_{60} cluster. Each number is an average over ten bonds. Numbers are unitless.

Fig. 8 Most stable structures for neutral metal clusters up to nine atoms.

Fig. 1(a)

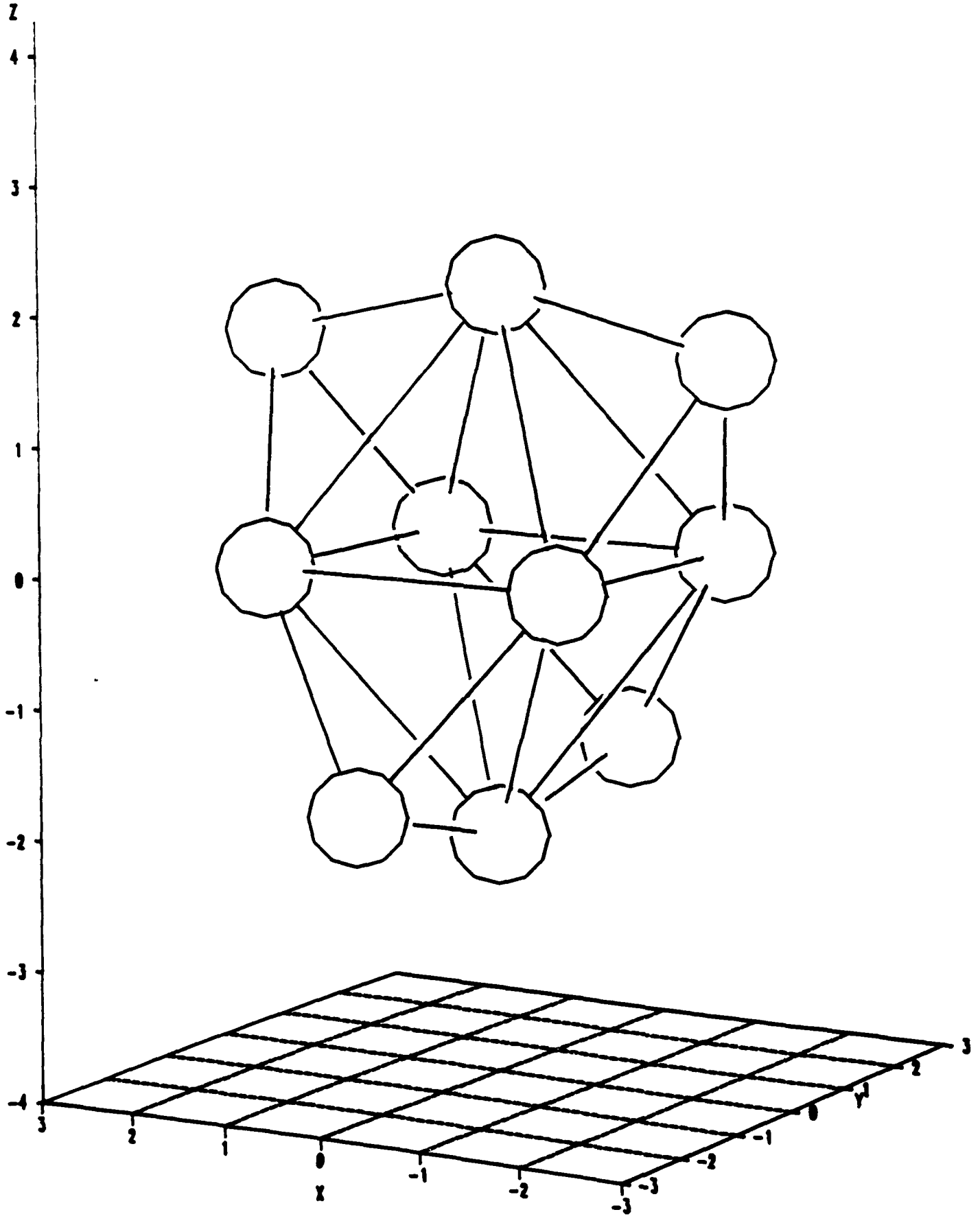

Fig. 1(b)

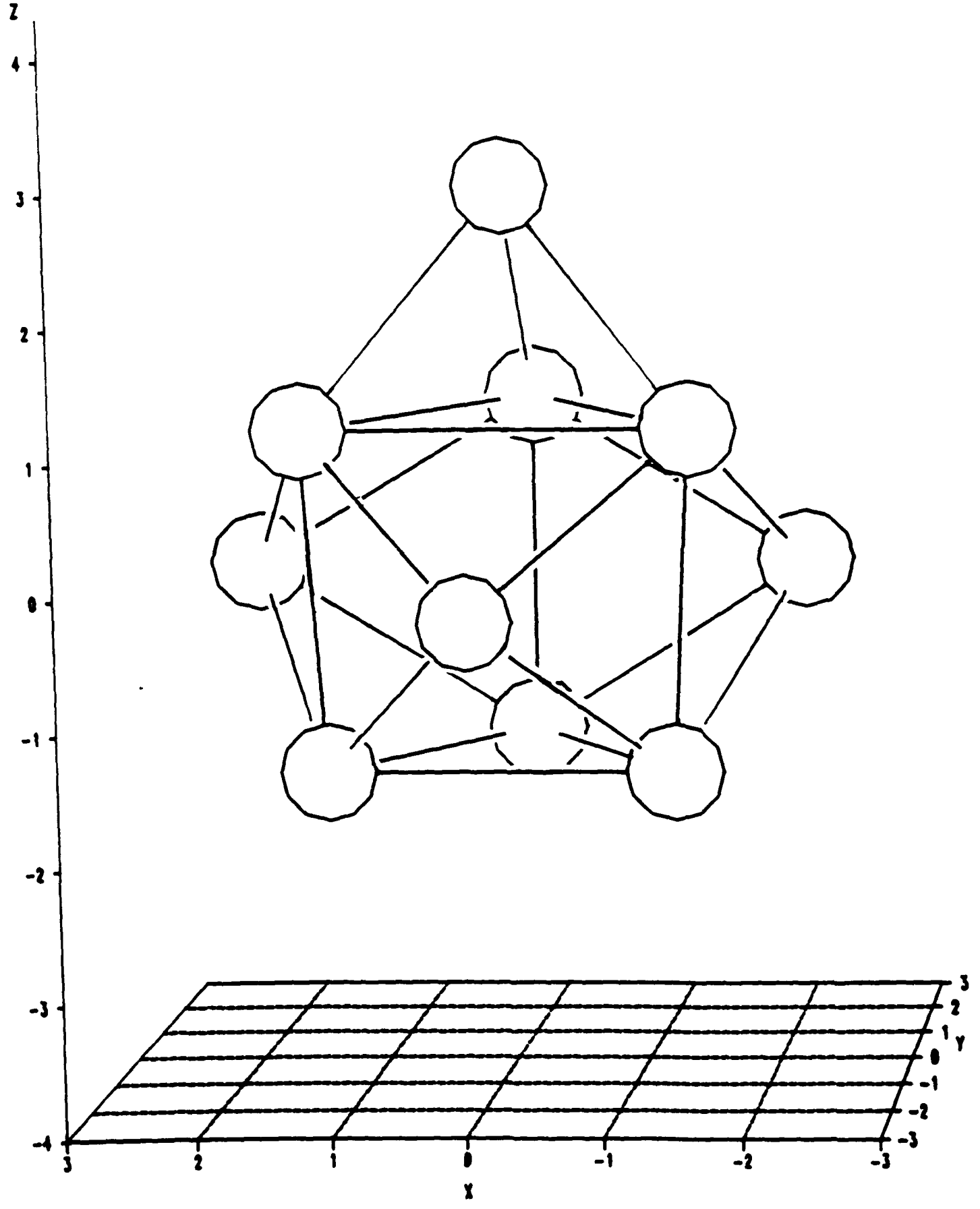

Fig 1(c)

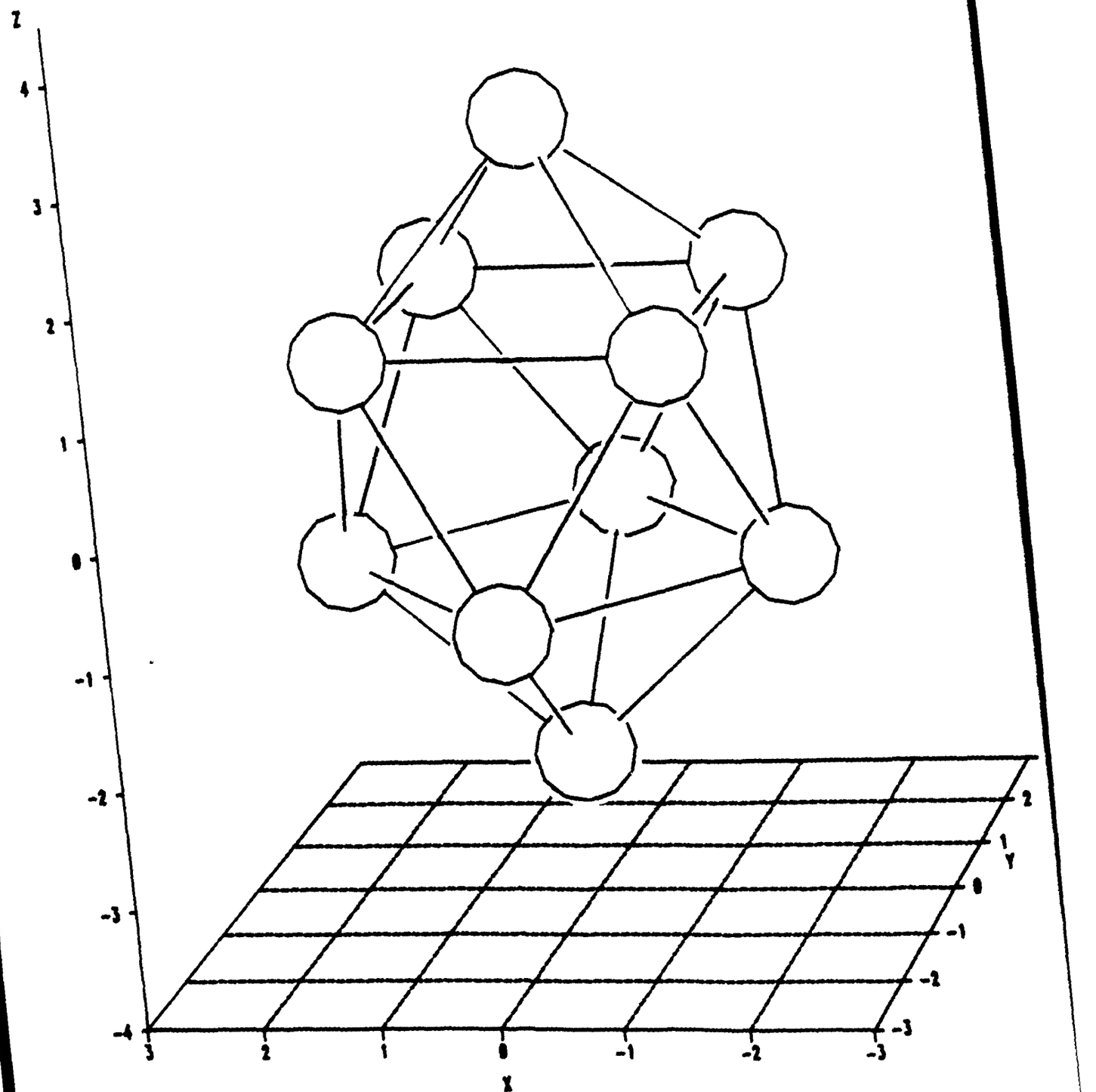

Fig. 1 (d)

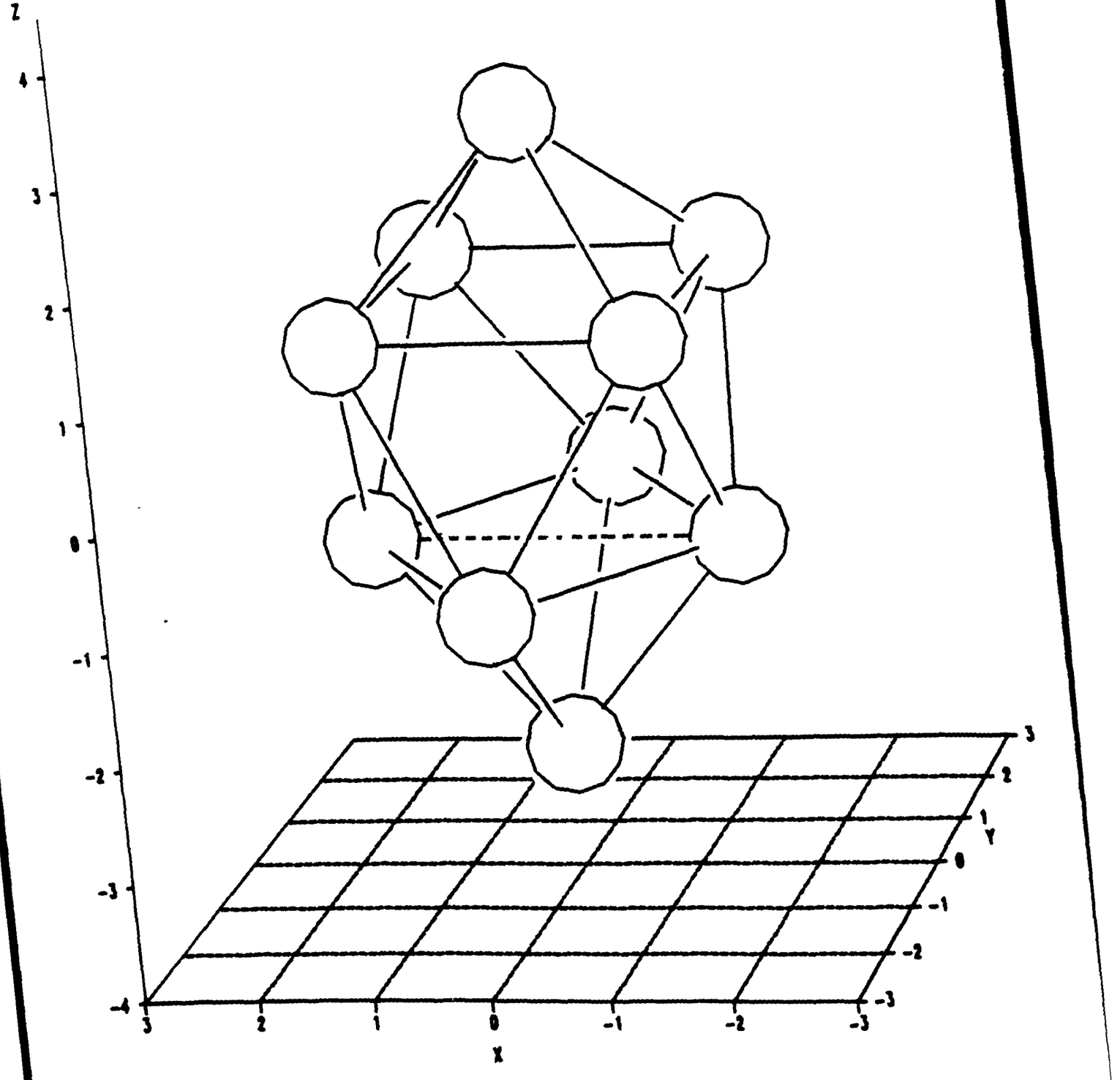

Fig. 2

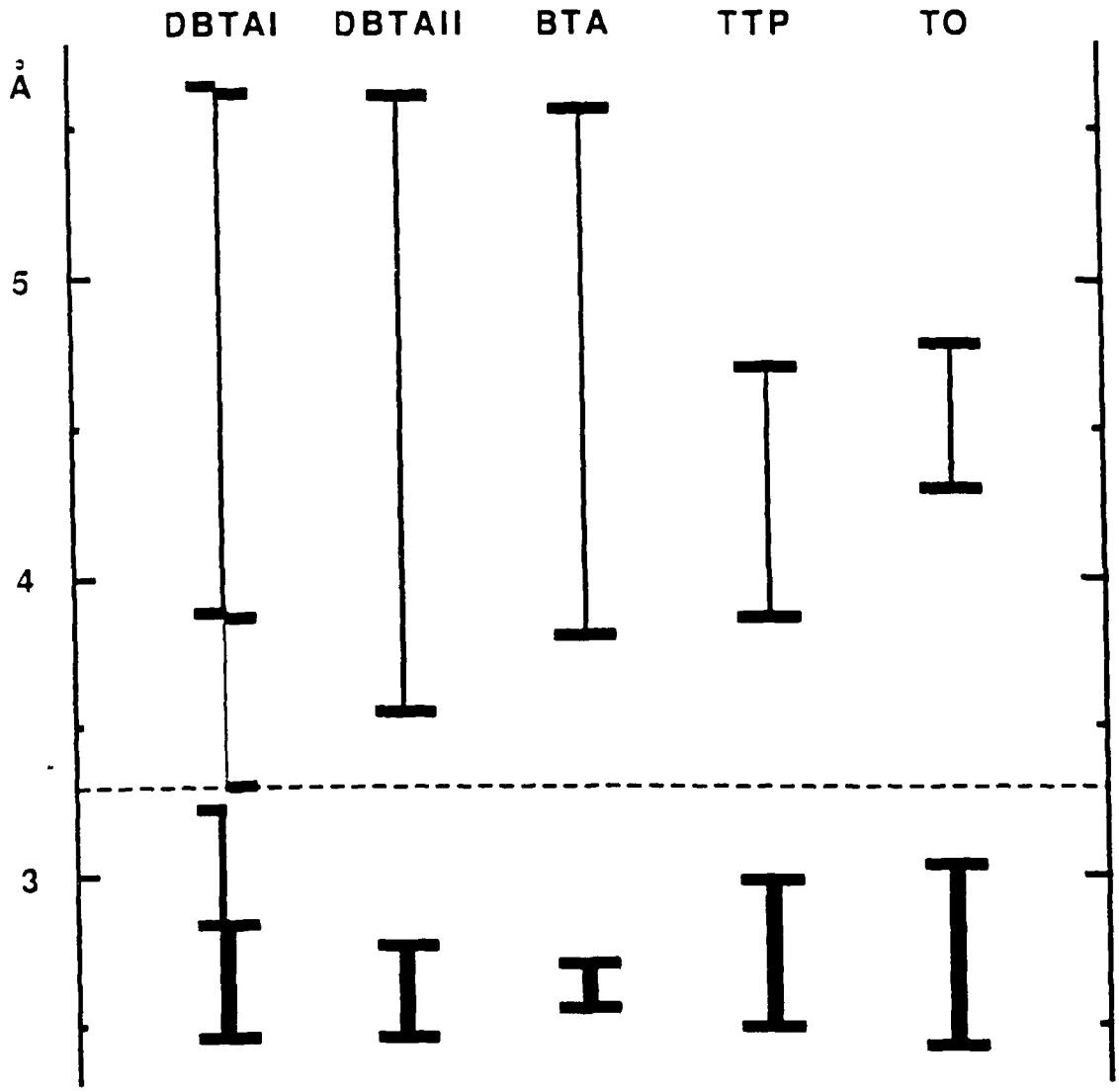

Fig. 3

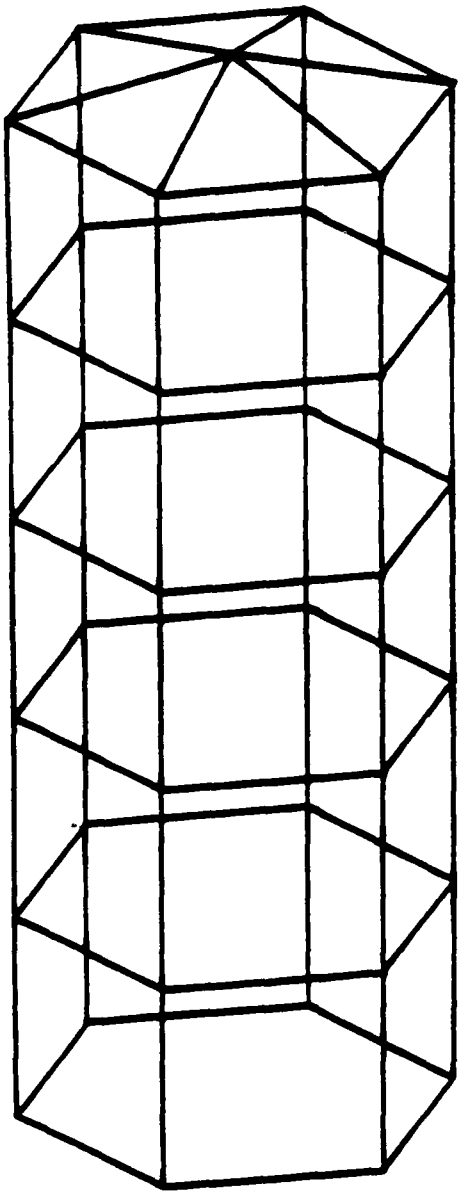

Si_{37}^{+}

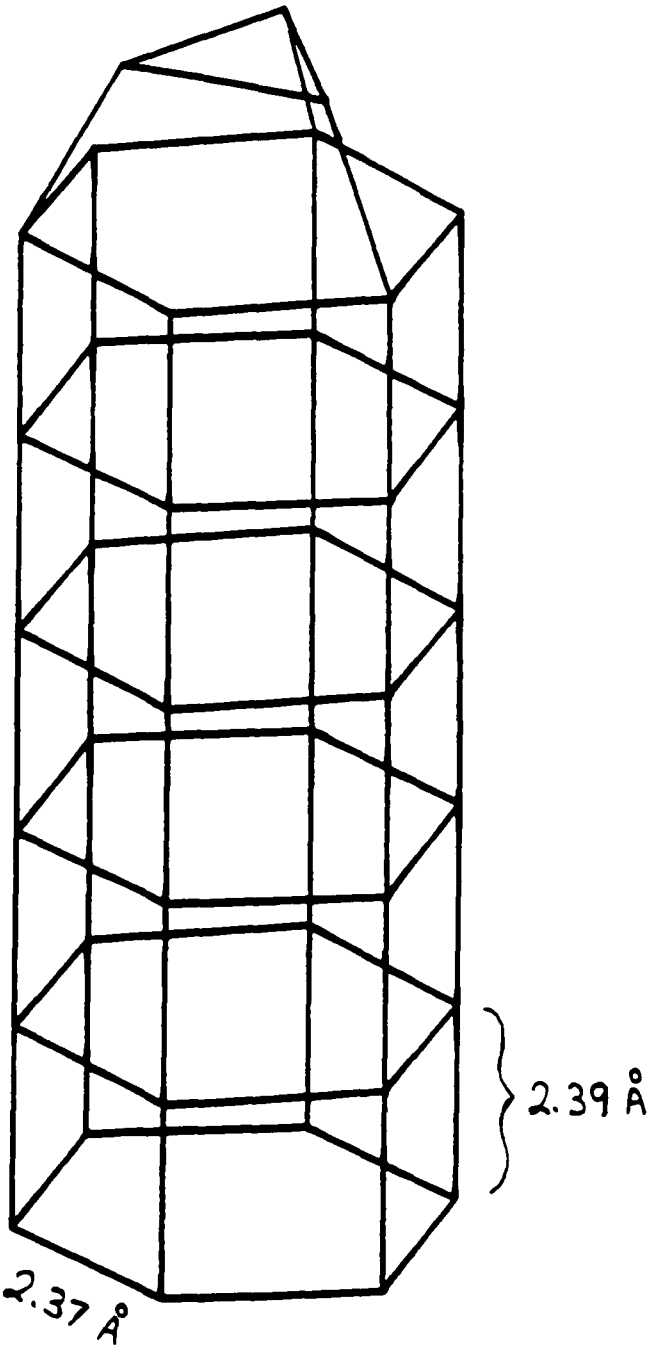

Si_{39}^{+}

Fig. 4

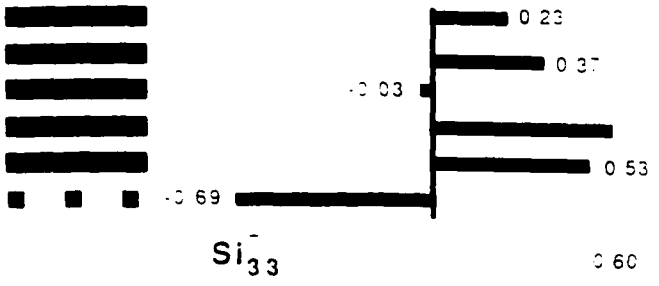

Si_{33}^-

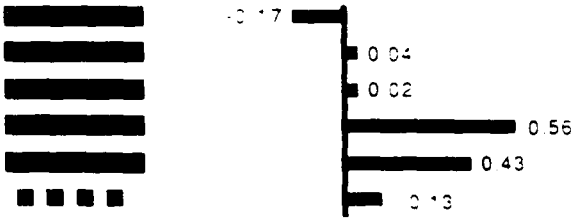

Si_{34}^-

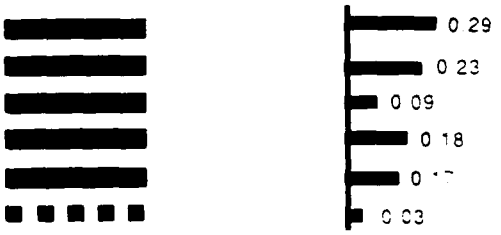

Si_{35}^-

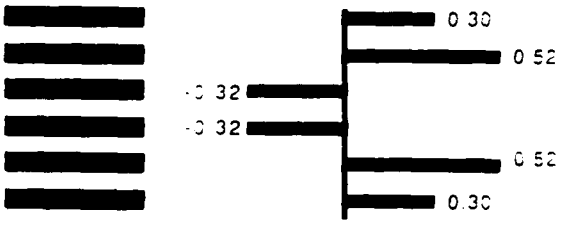

Si_{36}^-

Si_{37}^-

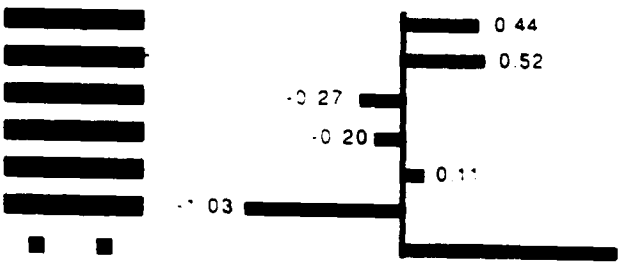

Si_{38}^-

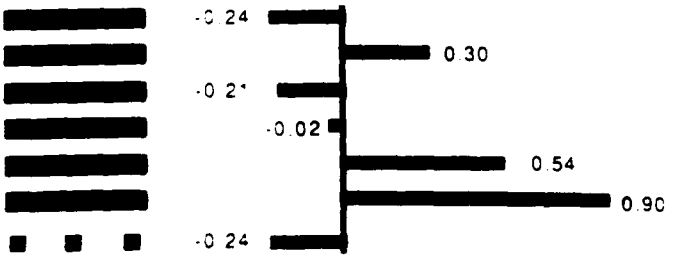

Si_{39}^-

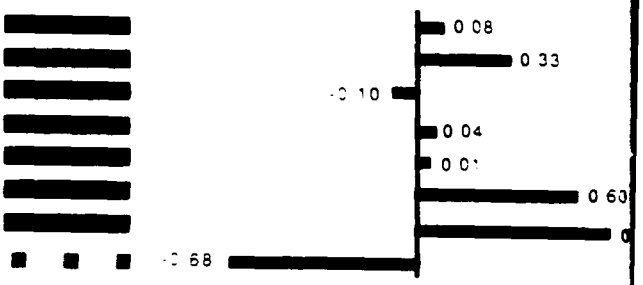

Si_{45}^-

Fig 5

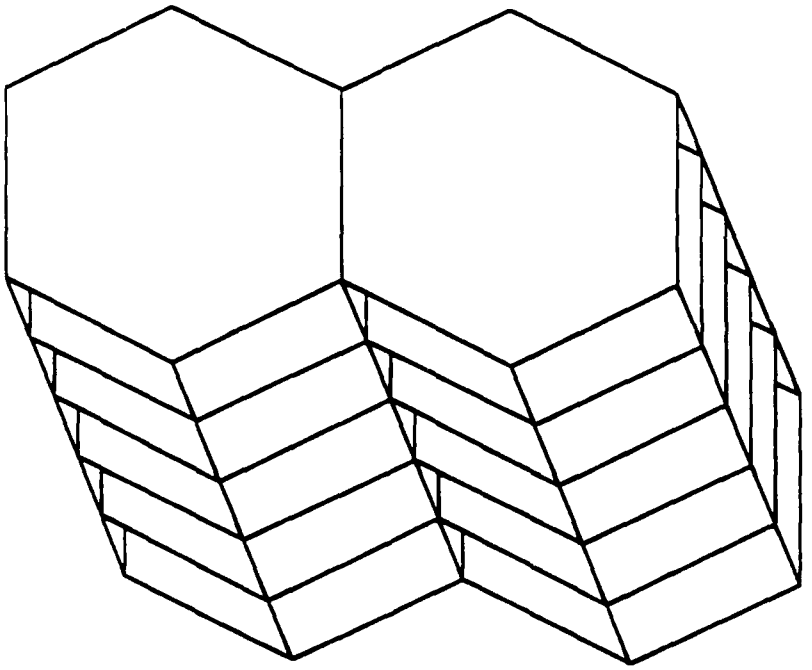

Fig 6

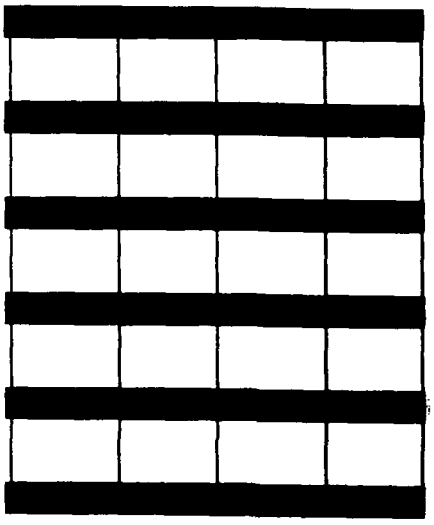

Fig. 7

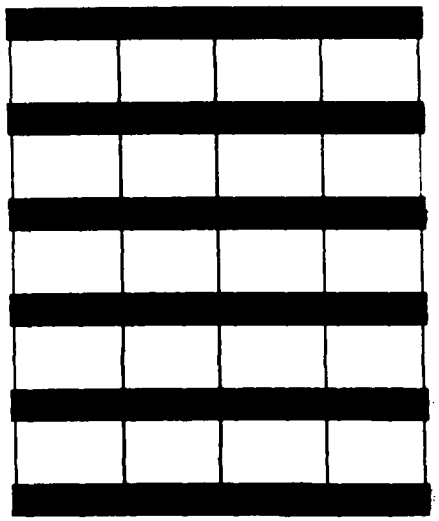

Fig. 3

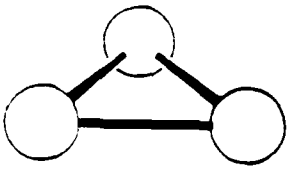

(a) M_3, D_{3h}

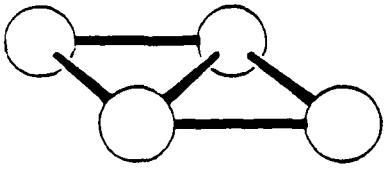

(b) M_4, D_{2h}

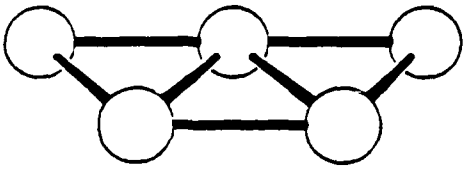

(c) M_5, C_{2v}

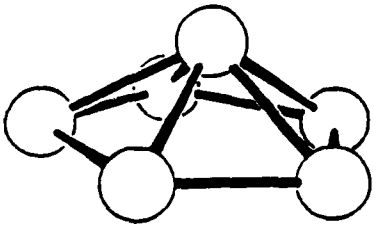

(d) M_6, C_{5v}

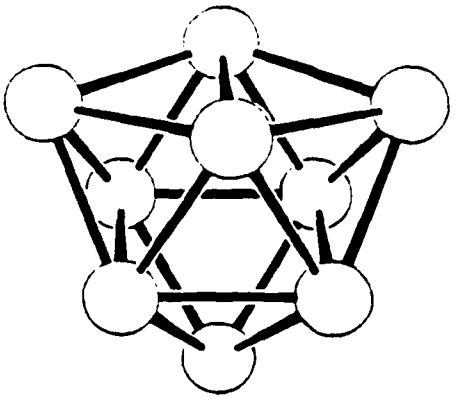

(g) M_9, D_{3h}

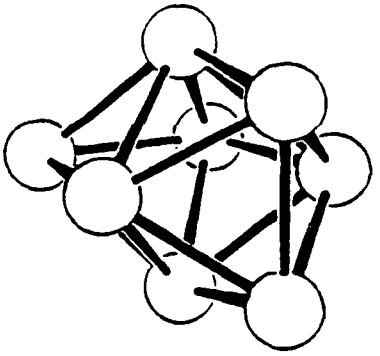

(f) M_8, D_{2d}

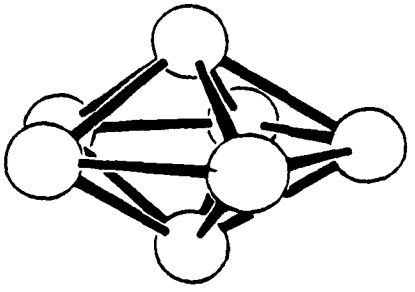

(e) M_7, D_{5h}

FY90 Abstracts Distribution List for Solid State & Surface Chemistry

Professor John Baldeschwieler
Department of Chemistry
California Inst. of Technology
Pasadena, CA 91125

Professor Paul Barbara
Department of Chemistry
University of Minnesota
Minneapolis, MN 55455-0431

Dr. Duncan Brown
Advanced Technology Materials
520-B Danury Rd.
New Milford, CT 06776

Professor Stanley Bruckenstein
Department of Chemistry
State University of New York
Buffalo, NY 14214

Professor Carolyn Cassady
Department of Chemistry
Miami University
Oxford, OH 45056

Professor R.P.H. Chang
Dept. Matls. Sci. & Engineering
Northwestern University
Evanston, IL 60208

Professor Frank DiSalvo
Department of Chemistry
Cornell University
Ithaca, NY 14853

Dr. James Duncan
Federal Systems Division
Eastman Kodak Company
Rochester, NY 14650-2156

Professor Arthur Ellis
Department of Chemistry
University of Wisconsin
Madison, WI 53706

Professor Mustafa El-Sayed
Department of Chemistry
University of California
Los Angeles, CA 90024

Professor John Eyler
Department of Chemistry
University of Florida
Gainesville, FL 32611

Professor James Garvey
Department of Chemistry
State University of New York
Buffalo, NY 14214

Professor Steven George
Department of Chemistry
Stanford University
Stanford, CA 94305

Professor Tom George
Dept. of Chemistry & Physics
State University of New York
Buffalo, NY 14260

Dr. Robert Hamers
IBM T.J. Watson Research Center
P.O. Box 218
Yorktown Heights, NY 10598

Professor Paul Hansma
Department of Physics
University of California
Santa Barbara, CA 93106

Professor Charles Harris
Department of Chemistry
University of California
Berkeley, CA 94720

Professor John Hemminger
Department of Chemistry
University of California
Irvine, CA 92717

Professor Roald Hoffmann
Department of Chemistry
Cornell University
Ithaca, NY 14853

Professor Leonard Interrante
Department of Chemistry
Rensselaer Polytechnic Institute
Troy, NY 12181

Professor Eugene Irene
Department of Chemistry
University of North Carolina
Chapel Hill, NC 27514

Dr. Sylvia Johnson
SRI International
333 Ravenswood Avenue
Menlo Park, CA 94025

Dr. Zakya Kafafi
Code 6551
Naval Research Laboratory
Washington, DC 20375-5000

Professor Larry Kesmodel
Department of Physics
Indiana University
Bloomington, IN 47403

Professor Max Lagally
Dept. Metal. & Min. Engineering
University of Wisconsin
Madison, WI 53706

Dr. Stephen Lieberman
Code 522
Naval Ocean Systems Center
San Diego, CA 92152

Professor M.C. Lin
Department of Chemistry
Emory University
Atlanta, GA 30322

Professor Fred McLafferty
Department of Chemistry
Cornell University
Ithaca, NY 14853-1301

Professor Horia Metiu
Department of Chemistry
University of California
Santa Barbara, CA 93106

Professor Larry Miller
Department of Chemistry
University of Minnesota
Minneapolis, MN 55455-0431

Professor George Morrison
Department of Chemistry
Cornell University
Ithaca, NY 14853

Professor Daniel Neumark
Department of Chemistry
University of California
Berkeley, CA 94720

Professor David Ramaker
Department of Chemistry
George Washington University
Washington, DC 20052

Dr. Gary Rubloff
IBM T.J. Watson Research Center
P.O. Box 218
Yorktown Heights, NY 10598

Professor Richard Smalley
Department of Chemistry
Rice University
P.O. Box 1892
Houston, TX 77251

Professor Gerald Stringfellow
Dept. of Matls. Sci. & Engineering
University of Utah
Salt Lake City, UT 84112

Professor Galen Stucky
Department of Chemistry
University of California
Santa Barbara, CA 93106

Professor H. Tachikawa
Department of Chemistry
Jackson State University
Jackson, MI 39217-0510

Professor William Unertl
Lab. for Surface Sci. & Technology
University of Maine
Orono, ME 04469

Dr. Terrell Vanderah
Code 3854
Naval Weapons Center
China Lake, CA 93555

Professor John Weaver
Dept. of Chem. & Mat. Sciences
University of Minnesota
Minneapolis, MN 55455

Professor Brad Weiner
Department of Chemistry
University of Puerto Rico
Rio Piedras, Puerto Rico 00931

Professor Robert Whetten
Department of Chemistry
University of California
Los Angeles, CA 90024

Professor R. Stanley Williams
Department of Chemistry
University of California
Los Angeles, CA 90024

Professor Nicholas Winograd
Department of Chemistry
Pennsylvania State University
University Park, PA 16802

Professor Aaron Wold
Department of Chemistry
Brown University
Providence, RI 02912

Professor Vicki Wysocki
Department of Chemistry
Virginia Commonwealth University
Richmond, VA 23284-2006

Professor John Yates
Department of Chemistry
University of Pittsburgh
Pittsburgh, PA 15260